Red Blood Cells Capture and Deliver Bacterial DNA to Drive Host Responses During Polymicrobial Sepsis

LK Metthew Lam[1], Nathan J. Klingensmith[2], Layal Sayegh[1], Emily Oatman[2] , Joshua S. Jose[1], Christopher V. Cosgriff [3], Kaitlyn A. Eckart[1], John McGinnis[1], Piyush Ranjan[4], Matthew Lanza[5], Nadir Yehya[6], Nuala J. Meyer[1,7], Robert P. Dickson[4,8,9], Nilam S. Mangalmurti[1,7]

Affiliations:
[1]Division of Pulmonary, Allergy, and Critical Care, Perelman School of Medicine at the University of Pennsylvania, Philadelphia, PA , USA
[2]Division of Traumatology, Surgical Critical Care and Emergency Surgery, Perelman School of Medicine at the University of Pennsylvania, Philadelphia, PA , USA
[3]Pulmonary and Critical Care Unit, Department of Medicine, Massachusetts General Hospital, Boston, MA, USA
[4] Division of Pulmonary and Critical Care Medicine, Department of Internal Medicine, University of Michigan Health System, Ann Arbor, MI, USA
[5]Department of Comparative Medicine, Penn State Health Milton S. Hershey Medical Center Hershey, PA USA
[6]Division of Pediatric Critical Care, Perelman School of Medicine at the University of Pennsylvania, Philadelphia, PA, USA
[7]Institute for Immunology, Perelman School of Medicine, University of Pennsylvania, Philadelphia, PA , USA
[8] Weil Institute for Critical Care Research & Innovation; Ann Arbor, Michigan
[9]Department of Microbiology and Immunology, University of Michigan Medical School, Ann Arbor, MI, USA

*Corresponding author: Nilam S. Mangalmurti
Stemmler Hall
Perelman School of Medicine
3450 Hamilton Walk
Philadelphia, PA 19104
215-573-9918
Email: nspatel@pennmedicine.upenn.edu

One Sentence Summary: RBCs modulate the host inflammatory response in sepsis

Conflict of interest statement: NSM is the founder of SENTICELL™ and the inventor on "Methods for Detection of Pathogenic Infections using Red Blood Cell-containing Patient Samples" (U.S. provisional patent application no. 63/022,181; PCT application no. PCT/US2021/031323; no 3178218, Canada, no. 218007516 Europe).

Abstract: Red blood cells (RBCs), traditionally recognized for their role in transporting oxygen, play a pivotal role in the body's immune response by expressing TLR9 and scavenging excess host cell-free DNA. DNA capture by RBCs leads to accelerated RBC clearance and triggers inflammation. Whether RBCs can also acquire microbial DNA during infections is unknown. Murine RBCs acquire microbial DNA in vitro and bacterial-DNA-induced macrophage activation was augmented by WT but not Tlr9-deleted RBCs. In a mouse model of polymicrobial sepsis, RBC-bound bacterial DNA was elevated in WT but not in erythroid Tlr9-deleted mice. Plasma cytokine analysis in these mice revealed distinct sepsis clusters characterized by persistent hypothermia and hyperinflammation in the most severely affected subjects. RBC-Tlr9 deletion attenuated plasma and tissue IL-6 production in the most severe group. Parallel findings in human subjects confirmed that RBCs from septic patients harbored more bacterial DNA compared to healthy individuals. Further analysis through 16S sequencing of RBC-bound DNA illustrated distinct microbial communities, with RBC-bound DNA composition correlating with plasma IL-6 in patients with sepsis. Collectively, these findings unveil RBCs as overlooked reservoirs and couriers of microbial DNA, capable of influencing host inflammatory responses in sepsis.

Introduction

Recognition of microbial-derived nucleic acid by cytosolic and endosomal receptors is vital for initiating inflammatory responses essential for host defense. We have recently discovered that mammalian red blood cells (RBCs) express the nucleic acid-sensing receptor TLR9 and can bind mitochondrial DNA, functioning as immune sentinels by triggering rapid senescence and loss of self, with consequent clearance and innate immune activation upon excess DNA binding.(1) Collectively, these findings suggest that circulating RBCs modulate host immune responses during inflammatory states, yet whether RBCs acquire bacterial DNA during sepsis remains unknown.

While elevated plasma cell-free CpG-containing mitochondrial DNA is a hallmark of critical illness syndromes, including sepsis and trauma, an emerging body of literature has demonstrated elevated bacterial DNA in the circulation during sepsis and pneumonia.(2, 3) In light of the accumulating evidence demonstrating the association of circulating microbial DNA and host inflammatory responses and the plausible interaction between RBCs and bacteria in the vascular compartment, we asked whether RBCs could acquire microbial DNA and orchestrate distinct host inflammatory responses.(4) In a murine model of polymicrobial sepsis we show that RBCs capture microbial DNA during sepsis and that RBC-Tlr9-mediated DNA delivery drives hyperinflammation. Moreover, RBCs from critically ill patients with sepsis harbor distinct microbial DNA composition compared to those from healthy donors, which correlate with the systemic inflammatory response. Thus, the process of RBC-mediated DNA capture and delivery shapes diverse host inflammatory responses during sepsis.

Results

CS injection recapitulates human sepsis features and RBC-bound bacterial DNA is elevated following CS-induced sepsis

Although no pre-clinical model can recapitulate all of the features of a clinical syndrome, the cecal slurry (CS) model of polymicrobial sepsis captures the hallmark features of sepsis, including organ dysfunction, temperature disruption, and cytokine storm.(5, 6) To investigate the role of RBC-DNA capture in sepsis, we induced CS sepsis in WT mice and mice in which Tlr9 was deleted in erythrocytes ($Ery^{tlr9-/-}$ mice). The baseline characteristics of the mice have been previously described(1) and are described in Supplemental Figure 1. Tlr9 is retained on immune cells in the $Ery^{tlr9-/-}$ mice (Supplemental Figure 1A-G) and we do not observe differences in baseline spleen and liver weight or RBC hemoglobin content (Supplemental Figure 1H-J). (1) CS injection induced weight loss and hypothermia in all mice (Figure 1A-C). At early time points but not later time points, $Ery^{tlr9-/-}$ mice demonstrated increased hypothermia when compared with WT mice (Figure 1B). Although a subset of WT mice never developed hypothermia, all $Ery^{tlr9-/-}$ mice developed hypothermia (Figure 1C, P=0.035). CS injection led to mortality in WT and $Ery^{tlr9-/-}$ mice, (Figure 1D). Bacterial dissemination was measured by quantifying colony-forming units (CFUs) in distant organs following CS injection. We observed increased spleen bacterial dissemination in $Ery^{tlr9-/-}$ mice compared to WT mice, P=0.03, Table 1.

We next examined the organs of mice subjected to the sepsis model 24 hours following CS injection. Consistent with previous reports, splenic injury was characterized by neutrophilic inflammation, lymphocyte death, and germinal hyperplasia (Supplemental Figure 2A&B, Supplemental Table 1). Liver injury, characterized by hepatocyte apoptosis, oval cell

hyperplasia, and focal necrosis, was also present (Supplemental Figure 2C&D, Supplemental Table 1). Notably, liver microabcesses were present in two of the Ery$^{tlr9-/-}$ mice but none of the WT mice.

We next asked if RBCs bound live bacteria following CS injection, RBCs were not associated with live bacteria as we could not culture bacteria from purified RBCs obtained from control or CS-injected mice (Supplemental Figure 2E). Because we had previously observed RBC acquisition of mtDNA during human and murine sepsis(1), we asked whether RBCs acquired bacterial DNA in a murine model of polymicrobial sepsis by performing qPCR for 16S on RBCs obtained from mice subjected to the cecal slurry model of sepsis. Consistent with our observation of increased mtDNA acquisition during sepsis, 16S was elevated on RBCs from WT mice but not Ery$^{tlr9-/-}$ mice six hours following the induction of CS-induced sepsis. RBCs from the Ery$^{tlr9-/-}$ mice did not acquire additional microbial DNA after CS injection, suggesting that RBCs may acquire microbial DNA during sepsis through Tlr9 (Figure 1E). While RBC-bound 16S significantly differed between WT and Ery$^{tlr9-/-}$ mice following CS-induced sepsis, plasma 16S was not significantly different between WT and Ery$^{tlr9-/-}$ mice (Supplemental Figure 2F).

Since we previously observed morphologic changes in human RBCs following excess DNA binding(1) and we detected elevated microbial DNA bound to RBCs during sepsis, we asked if RBC morphology is altered following the induction of CS-induced sepsis. Notably, Ery$^{tlr9-/-}$ RBCs remained morphologically intact, whereas echinocytes and loss of biconcave shape were observed in WT RBCs (Figure 1F and G). These findings indicate that RBC morphological changes observed during sepsis are influenced by RBC-Tlr9. We also measured cell-free hemoglobin which has been shown to increase tissue injury following polymicrobial sepsis.(7)

Plasma cell-free hemoglobin was elevated in Ery$^{tlr9-/-}$ but not WT mice following CS-induced sepsis (Figure1H).

Host Cytokine Responses are Heterogenous and Dependent on RBC-Tlr9

Next, we measured plasma cytokines following CS injection. We observed heterogeneity in plasma cytokine production in the CS-injected mice (Figure 2A). To better dissect the heterogeneity observed, we applied uniform manifold approximation and projection (UMAP) in order to visualize the nine measured cytokines in a two-dimensional space. Three distinct clusters emerged in this projection, which discriminated between persistent temperature phenotype and controls (Figure 2B). Cluster 1 was defined by persistent hypothermia and associated with increased organ dissemination and elevated plasma cytokines (Figure 2B, Supplemental Figure 3). Cluster 2, was defined by transient hypothermia and was associated with decreased organ dissemination and decreased cytokine production (Figure 2B, Supplemental Figure 3). Temperature trajectories for individual mice in the different treatment groups shown in Figure 1B are replotted in Supplemental Figure 3A. To visualize the relative concentration of the cytokines in each cluster, we fit a kernel density estimator to the UMAP space weighted by each of the log-normalized features revealing Cluster 1 to be enriched with the proinflammatory cytokines (Figure 2C). Agglomerative clustering on the nine cytokines recovered the same clusters (Figure 2D) and exemplified that there were two distinct cytokine expression patterns in response to the same insult, and these patterns correlated well with the temperature response phenotype.

Having identified this temperature response cluster, we re-classified mice on this clinically identifiable trait and compared the cytokine response by strain within each group. Analysis based on the hypothermic cluster revealed aberrant cytokine production in the persistently hypothermic Ery$^{tlr9-/-}$ mice when compared with persistently hypothermic WT mice. We observed attenuated plasma IL-6, IL-10, and IL-1β in the Ery$^{tlr9-/-}$ mice compared to WT mice (Figure 2E). Spleen and liver cytokine transcripts were examined by qPCR. In the spleen we observed attenuated IL-6 and IL-10, while in the liver we observed attenuated IL-6, IL-1β and IL-10 production (Figure 2F-I). Spleen IL-12 family cytokines transcripts were also attenuated in the Ery$^{tlr9-/-}$ mice (Supplemental Figure 3C). Because the erythropoietin receptor is present on some non-erythroid populations including red pulp macrophages (RPM) and we observed striking differences in dissemination and cytokine production in the spleens between WT and Ery$^{tlr9-/-}$ mice, we analyzed red pulp macrophages from WT and Ery$^{tlr9-/-}$ mice to ascertain whether *tlr9* was deleted in RPM.(8) As seen in Supplemental Figure 1G, RPMs in Ery$^{tlr9-/-}$ mice did not demonstrate a reduction in *tlr9*. Thus, the differences in dissemination and tissue cytokine production appear to be a result of RBC-Tlr9 deletion.

We examined correlations between tissue and plasma cytokines to determine if plasma cytokines reflect tissue cytokine production. Plasma IL-6, TNFα, and IL-10 correlated with spleen and liver cytokine generation (Supplemental Table 2). However, spleen and liver IL-1β were concordant with plasma levels in WT but not Ery$^{tlr9-/-}$ mice, and tissue IFNγ was discordant with plasma in both WT and erythroid Tlr9 deficient mice (Supplemental Table 2), suggesting that plasma IFNγ may not be a surrogate for tissue-level pathology during sepsis. Because we observed differences in organ dissemination between WT and Ery$^{tlr9-/-}$ mice, we next asked

whether tissue cytokines correlated with bacterial dissemination in remote organs in WT and Ery$^{tlr9\ -/-}$ mice. We observed significant correlations between tissue dissemination and cytokines in the spleen and liver of WT and Ery$^{tlr9-/-}$ mice. However, the cytokine and bacterial dissemination correlations differed between the two groups (Figure 2G and I) with significant associations between tissue IL-6 and IL-1β cytokine production and dissemination observed in WT but not Ery$^{tlr9-/-}$ mice. Collectively, these findings suggest that RBC-Tlr9-mediated DNA delivery may contribute to the heterogeneous host responses to identical stimuli.

RBCs deliver DNA to immune cells, initiating inflammatory responses

To validate our observations in the sepsis model, we asked whether RBCs could increase the delivery of microbial DNA to immune cells. We first assessed the ability of RBCs to sequester pathogen-derived DNA; RBCs were incubated with known quantities of bacterial DNA and then assayed for bacterial DNA acquisition by qPCR. In vitro, murine RBCs bound genomic DNA from common bacterial pathogens (Supplemental Figure 4A). We next treated peritoneal macrophages with genomic DNA from Staphylococcus aureus (Sa), Pseudomonas aeruginosa (PsA), or the immunostimulatory ODN, CpG 1826 or DNA-treated WT or Tlr9 deficient RBCs. Microbial DNA alone did not result in macrophage activation as measured by TNFα secretion. While microbial DNA alone did not lead to TNFα release, Sa DNA carrying WT RBCs but not Sa-DNA treated Tlr9 deficient RBCs induced robust TNFα secretion (Figure 3A), likewise PsA DNA alone did not result in macrophage activation and TNFα release. However, immunostimulatory CpG did result in robust macrophage activation. WT RBCs but not Ery$^{tlr9-/-}$ RBCs augmented CpG-mediated macrophage activation. To verify that our findings were not due to the inflammatory effects of heme, we measured cell-free hemoglobin in the supernatant of

RBC-treated macrophages. We did not observe increased hemolysis in the microbial DNA-treated RBC group, Supplemental Figure 4B.

We previously found that CpG-treated RBCs can trigger innate inflammatory responses in naïve mice.(1) We now asked whether RBC Tlr9 mediated DNA delivery to remote organs in naïve mice. WT RBCs and Tlr9 KO RBCs alone did not lead to liver inflammation as measured by increased neutrophil recruitment, while CpG did lead to increased liver neutrophil recruitment. CpG-treated WT RBCs increased liver neutrophils when compared with RBCs or CpG alone, while CpG-treated Tlr9 KO RBCs did not increase liver neutrophil recruitment (Figure 3B and C). These data would suggest that RBCs through Tlr9 can deliver immunostimulatory DNA to remote organs, triggering inflammatory cell recruitment. Consistent with these results, infusion of CpG-treated Tlr9 KO RBCs resulted in decreased plasma IL-6 production when compared with infusion of CpG-treated WT RBCs. (Figure 3D). Collectively, these findings suggested that RBCs are capable of supplying microbial DNA to immune cells and inciting inflammatory cytokine production.

RBC-bound microbial DNA community richness but not DNA burden correlates with IL-6 in human sepsis

To determine whether our pre-clinical observations of RBC-mediated immunoregulation through DNA-binding and delivery are germane to human sepsis, we asked whether human RBCs are associated with microbial DNA in health and in sepsis (Figure 4). First, we incubated human RBCs with *Legionella* sp. DNA in vitro to confirm that human RBCs are capable of binding bacterial DNA. When we assayed these RBCs using 16S rRNA gene amplicon sequencing,

97.5% (SD 1.5%) of all RBC-associated sequences were classified as *Legionella* sp. (Figure 4A). We thus concluded that human RBCs are capable of binding bacterial DNA and being assayed via 16S rRNA gene amplicon sequence.

We next investigated the *quantity* and *diversity* of bacterial DNA associated with human RBCs using qPCR of the bacterial 16S gene. As shown in Figure 4B, human RBCs contained more detectable bacterial DNA than our negative controls (buffer controls, $P<0.0001$, sterile water, $P<0.0001$). When we compared the quantity of bacterial DNA detected on RBCs from patients with and without sepsis, we found a greater quantity of bacterial DNA on RBCs from patients with sepsis, Figure 4B. Baseline characteristics of the sepsis cohort are found in Table 2. Next, using 16S rRNA gene amplicon sequencing, we compared the *community diversity* of bacterial DNA associated with human RBCs. As shown in Figure 4C, community diversity (both as measured using the Shannon Diversity Index and by community richness) was greater in human RBC-associated bacterial DNA than in negative control specimens. Neither diversity index differed across humans with and without sepsis. We thus concluded that human RBCs contain more bacterial DNA and greater bacterial diversity than do background control specimens, and the quantity of RBC-associated bacterial DNA is greater in sepsis than in health.

We then assessed the *community composition* of bacterial DNA detected in association with human RBCs (Figure 4D-F). Whether visualized via principal components analysis (Figure 4D) or rank abundance (Figure 4E) or tested using permutational multivariate ANOVA (PERMANOVA), we found distinct bacterial communities when comparing negative controls and human RBCs, both in health and sepsis ($P<0.0001$ for both, PERMANOVA). Communities

detected in RBCs from healthy subjects differed from those detected in RBCs from subjects with sepsis (P=0.007, PERMANOVA). As shown via rank abundance analysis (Figure 4E), some contaminant taxa detected in negative controls (e.g., *Comamonadaceae*) were detected in RBCs from healthy patients and patients with sepsis, though at a lower relative abundance (>50% in negative controls vs 10-15% in RBC specimens). In contrast, numerous taxa were detected in RBC-associated communities that were minimally present in negative controls (e.g., *Pseudomonadaceae*, *Mycobacteriaceae*). We thus concluded that while, as a low-biomass specimen, bacterial DNA associated with human RBCs is vulnerable to sequencing contamination, it also has a distinct bacterial signature that cannot be wholly explained via contamination.

Next, we determined the source of this distinct bacterial signal in RBC-associated bacterial DNA (Figure 4F). We directly compared prominent bacterial families detected in RBCs, as compared to negative control specimens, grouped by probable source community. Much of the bacterial signal was suspicious for procedural or sequencing contamination, evidenced by the high relative abundance of *Comamonadaceae* spp. (detected in negative controls) and *Flavobacteriaceae* spp. (minimally present in negative controls but taxonomically suggestive of an occult source of contamination). However, we found some bacterial taxa enriched in RBC-associated DNA suggestive of probable gut origin (e.g., *Lachnospiraceae*, *Clostridiaceae*, and *Enterococcaceae* spp.). Finally, some bacterial taxa were classified as potential pathogens (e.g., *Pseudomonadaceae* spp., *Staphylococcaceae* spp., *Streptococcacaeae* spp., *Actinomycetaceae* spp., and *Mycobacteriaceae* spp.). Of these, *Streptococcacaeae* spp., *Actinomycetaceae* spp., and *Mycobacteriaceae* spp. were most enriched in RBCs from sepsis patients relative to those from

healthy subjects. Importantly, among sepsis patients, neither the diversity, quantity, or community composition of RBC-associated bacterial DNA differed across patients with and without culture-identified bacteremia (Supplemental Figure 5, $P>0.05$ for all comparisons).

We next compared RBC-associated microbiota with patients' plasma concentrations of IL-6. We found that the community richness of RBC-associated bacterial DNA (the number of unique bacterial taxa detected) was positively correlated with patients' IL-6 concentrations, explaining 12% of patient variation in this inflammatory cytokine (Figure 4G). Using PERMANOVA, we found that the community composition of RBC-associated bacteria was correlated with patients' IL-6 concentrations, both at the OTU and family level of taxonomic classification ($P = 0.03$ and 0.01, respectively). The association between RBC-associated bacterial DNA diversity and plasma IL-6 remained significant after adjusting for vasopressor use and severity of illness (Figure 4G).

Taken together, we concluded that human RBCs are capable of binding bacterial DNA and contain a greater quantity and diversity of bacterial DNA than negative control specimens. The identity of RBC-associated bacterial DNA is influenced – but not entirely explained by – procedural and sequencing contamination, and the identity of bacterial DNA in RBCs from patients with sepsis differs from that of healthy subjects and is correlated with systemic IL-6 concentrations.

Discussion

In this study, we identify RBCs as critical regulators of the host inflammatory response during sepsis. Using a pre-clinical model of sepsis and genetic deletion of erythrocyte *Tlr9*, we demonstrate that circulating red cell-mediated DNA delivery drives heterogeneous host inflammatory responses through DNA capture and delivery to remote organs. In vitro, RBCs bind microbial DNA and increase DNA delivery to phagocytes triggering inflammation. Moreover, RBCs from patients with sepsis reveal distinct microbial DNA profiles and we identify red blood cells as a distinct reservoir for microbial DNA. These data demonstrate a previously unknown role for circulating RBCs as couriers of microbial DNA, capable of inciting heterogeneous host inflammatory responses during sepsis.

There is renewed interest in anti-inflammatory treatments for sepsis following the recent success of anti-inflammatory treatments for COVID-associated sepsis and ARDS.(9-11) Clinical trials of anti-IL-6 and re-analysis of IL-1RA for sepsis have yielded insight into the importance of these pathways in the host inflammatory response to pathogens in specific subsets of patients.(12) However, large trials of anti-inflammatories for sepsis have yet to show a mortality benefit. Discussions surrounding the failure to translate pre-clinical trials to successful therapies for sepsis have centered around the heterogeneous nature of this clinical syndrome and the inability of animal models to fully demonstrate the clinical features of this complex syndrome. Thus, animal modeling of clinical syndromes such as sepsis has been intensely scrutinized.(13) Identifying novel mechanisms that trigger inflammation within sepsis patients offers the promise of precision-medicine-based approaches for this complex syndrome. Here, using a pre-clinical model of sepsis, erythroid TLR9 deficient mice, in vitro studies, and human subjects, we

demonstrate that animal models can recapitulate key clinical features of sepsis and even provide insight into heterogeneous host responses. There was heterogeneity in the inflammatory response to CS injection in wild-type and in Ery$^{tlr9-/-}$ knockout mice. However, further studies will be required to elucidate additional mechanisms contributing to the heterogenous response to an identical stimulus. Notably, distinct differences in the tissue and systemic inflammatory cytokine production were observed in the absence of RBC-TLR9 in the persistently hypothermic cluster. This observation implies that the mechanism of red blood cell-mediated DNA delivery plays a significant role in eliciting part of the host's inflammatory response in this severe cluster. These observations were only possible after our unbiased analysis of plasma cytokines demonstrated differential clustering based on the persistent hypothermic response leading to a re-analysis of subjects in this temperature group. These findings are consistent with recent reports suggesting temperature trajectories predict clinical outcomes.(4, 14) Together, these results underscore the critical role of pre-clinical models in identifying mechanistic elements (ie RBC-TLR9) that may drive differential host inflammatory responses and identify RBC-TLR9 mediated DNA regulation as a potentially treatable trait in sepsis.

In the polymicrobial sepsis model, we observed a significant reduction in cytokine production in the plasma and spleen, alongside increased organ dissemination in mice that lacked erythrocyte Tlr9. Interestingly, plasma cell-free hemoglobin was elevated in the Ery$^{tlr9-/-}$ mice, which may have contributed to increased bacterial dissemination observed in this group. We recently demonstrated that human RBCs acquiring CpG-DNA become resistant to osmotic lysis.(1) In this in vivo model of polymicrobial sepsis, we now show that WT but not Ery$^{tlr9-/-}$ mice acquire microbial DNA and undergo echinocytosis. Whether microbial DNA acquisition of microbial

DNA and subsequent echinocytosis by RBCs confers resistance to hemolysis remains an active area of investigation.

In vitro experiments showed that WT red blood cells could activate macrophages in the presence of bacterial DNA, whereas RBCs from erythrocyte-specific Tlr9 knockout ($Ery^{tlr9-/-}$) mice did not. These data indicate that Tlr9-mediated DNA delivery by RBCs plays a crucial role in regulating the host's inflammatory response. Additionally, in a focused model examining DNA delivery by RBCs, the absence of RBC Tlr9 impaired neutrophil recruitment to the liver following systemic DNA administration. Collectively, these findings underscore the importance of early RBC-mediated DNA delivery in driving the host inflammatory response. A failure in this process, as observed in the absence of RBC-Tlr9, resulted in attenuated cytokine responses and inflammatory cell recruitment, impairing microbial control.

We observed consistent findings in our clinical cohort where red-cell-associated microbial DNA community richness correlated with IL-6, suggesting that RBC-mediated DNA delivery is a driver of the IL-6 response at the tissue level. In addition, we have previously demonstrated that critically ill patients with sepsis demonstrate elevated surface RBC-TLR9 and diversity in surface RBC-TLR9 expression.(1) These findings lead us to speculate that RBCs contribute to the host inflammatory response and IL-6 signaling and may contribute to host diversity through intrinsically distinct DNA binding capabilities. However, further studies of RBC heterogeneity and surface TLR9 expression in more extensive cohorts will be needed to validate this hypothesis.

Our data show that RBCs can avidly bind microbial DNA from multiple pathogenic organisms in vitro. Furthermore, RBCs acquire microbial DNA in a murine model of polymicrobial sepsis and a cohort of critically ill septic patients. We have previously reported that RBCs sequester mitochondrial DNA during non-COVID and COVID sepsis and that RBC-bound mtDNA is associated with anemia.(1, 15) Sequestration of mtDNA was not unexpected as numerous studies have demonstrated the presence of elevated cell-free mtDNA in the plasma of critically ill patients.(16, 17) One study, however, has linked the presence of bacterial DNA in the circulation with outcomes in critically ill patients with COVID-19.(18) The detection of bacterial DNA bound to RBCs in patients with culture-negative sepsis was an unexpected finding but consistent with the literature that demonstrates the presence of cf-bacterial DNA in the circulation of patients with culture-negative sepsis.(19-21) Consistent with these findings, others have found bacterial DNA present in remote organs, including the brain and lung, during sepsis, suggesting that gut microbial translocation contributes to organ injury during sepsis. (22-24)

Although we observed increased 16S DNA on RBCs from septic patients when compared with healthy donors, the detection of microbial DNA present on RBCs in the healthy donors suggests that another homeostatic role of RBCs may be to scavenge microbial DNA from the gut or other tissues. Given, the ample evidence for microbial translocation into the circulation during routine tasks such as tooth brushing, exercise, and simply aging (25-28), it is plausible that RBCs may serve to sequester microbial DNA under basal conditions. Currently, the origin of RBC-bound microbial DNA remains enigmatic. Given that RBCs circulate through all tissues, we hypothesize several potential sources of RBC-bound microbial DNA, including direct acquisition from infected tissue sites, uptake of microbial DNA from the circulation during infection, and

intermittent transfer of bacteria through common sources of transient bacteremia. Our studies, comparing bacterial density, diversity, and community composition in patients with both sepsis and culture-negative sepsis, revealed no significant differences. This finding challenges the assumption that bacteremia is the primary source of RBC-bound microbial DNA. In our cohort, probable pathogens constitute only a small portion of the RBC-enriched taxa. We hypothesize that RBC-bound bacterial DNA may represent bacterial DNA accumulated over the lifespan of the RBCs as the RBC-bound DNA is not dominated by the disseminated pathogens. Our findings suggest that the RBCs are not just scavenging pathogen DNA in bacteremic patients but may instead reflect the cumulative bacterial DNA acquired by the RBCs over their 120-day lifespan. Thus, as opposed to a model in which RBC-associated 16S signal identifies acutely disseminated pathogens, we instead hypothesize that RBCs may serve as a circulating "sponge" that acquires bacterial DNA present in the blood throughout its 120-day lifetime. While the temporal dynamics of RBC-associated microbial DNA (including degradation and turnover) have yet to be determined, we believe this hypothesis could explain the multiple likely anatomic sources of RBC-associated microbial DNA (Figure 4) and is congruent with our hypothesis that RBCs serve as DNA traffickers via a TLR9-dependent mechanism. Thus, RBC-associated bacterial DNA may instead represent evidence of a regulated, homeostatic process (the host calibrating its systemic immune tone based on the density and identity of intermitted bacteria or bacterial egress from any source) as opposed to a mere artifact of overwhelming infection. This leads us to surmise that the association of bacterial DNA with RBCs may be part of a regulated homeostatic mechanism, wherein the host adjusts its systemic immune response based on the nature of bacteria acquired from these diverse sources. Although speculative at this time, such a mechanism, if confirmed, could redefine our understanding of the interplay between microbial

exposure during homeostasis and systemic immune modulation. It is thus not surprising that healthy donors and septic patients exhibited a large amount of nucleic acid on their RBCs. The latter likely reflects the ability of RBCs to sequester DNA from the immediate environment, further supporting the hypothesis that RBCs function to maintain homeostasis by continually scavenging cf-DNA(15). During infection, however, we have recently found that excess CpG-binding leads to innate immune activation and inflammation, and others have validated these findings, demonstrating the immunogenicity of CpG-loaded RBCs using in vivo tumor models(1, 29). Our current observations suggest that during sepsis, in the presence of excess bacterial DNA, RBCs deliver DNA to remote organs, driving inflammation.

RBC-based diagnostics may provide insight into inflammation and injury at the tissue level that is not obtainable from plasma. There is potential that this methodology might lead to novel detection strategies for pathogens using small volume samples as we detected a high abundance of microbial DNA from just 10^7 RBCs (~ 2uL of RBCs). Identifying an easily accessible, low-volume, high-mass template for molecular diagnostics represents a fundamental breakthrough in pathogen diagnostics. However, as it currently stands, the 16S rRNA bacterial gene sequencing is not an optimal platform to interpret the microbial signal present on RBCs and translate it into actionable bedside information. This is likely for several reasons. One is that despite a high bacterial signal on the RBCs, finding pathogenic DNA appears to be a needle in the haystack problem. The amount of DNA might be overwhelmed by the other more predominant bacterial nucleic acids as described above. Secondly, there is no guarantee that if pathogen DNA is sequestered on the RBC surface, it will be the 16S rRNA gene fragment, future studies targeting the entire microbial genome to examine RBC-bound microbial DNA will be required to

overcome this limitation. Additionally, due to the long lifespan of RBCs, it is plausible that microbial DNA associated with the RBCs detected by sequencing reflects cumulative microbial DNA present over the lifespan of the RBC (~120 days). As evidenced by our 16S rRNA gene analysis of human RBCs, this low-biomass specimen is also vulnerable to procedural and sequencing contamination. Hence, in the context of diagnostics, the application of RBC-based 16S sequencing is currently considered to have limited effectiveness. Future research focusing on targeted qPCR for detecting RBC-bound pathogens may be more beneficial.

While the quantity of 16S bound to RBCs did not associate with inflammatory cytokines in patients, *community composition* and *richness* of RBC-associated microbial DNA did associate with IL-6. Further in vitro mechanistic studies will be needed to interrogate the hypothesis that RBC-bound microbial DNA composition differentially regulates host inflammatory responses including phagocyte cell death. Our clinical observations of RBC-bound DNA associated with inflammation are validated in the pre-clinical animal model, where we demonstrate that loss of RBC-TLR9 attenuates end-organ IL-6 and IL-1B production in severely ill animals. However, our study has limitations. While our preclinical data suggest that RBCs can deliver CpG-DNA to remote organs, in this single-center, small cohort, we were only able to show an association between RBC-bound microbial DNA diversity and plasma IL-6 levels. Larger studies will be necessary to further elucidate the role of RBC-mediated microbial DNA regulation in influencing host inflammatory responses in patients with sepsis

In this study, we uncover a non-gas exchanging function of RBCs as couriers of microbial DNA through TLR9. Our findings show that RBC-mediated DNA transport elicits specific host

responses in a preclinical sepsis model and RBC-bound microbial DNA associated with systemic inflammation in sepsis patients, offering new insights into previously unexplored mechanisms contributing to the heterogenous host response in sepsis. Additionally, RBCs emerge as an unexpected reservoir for microbial DNA that may be exploited in the future to develop molecular diagnostics for infectious diseases. Collectively, we identify a critical role for circulating RBC-TLR9 in modulating the host inflammatory responses during sepsis, highlighting their dual function as both reservoirs and couriers of microbial DNA.

Methods

Sex as a biological variable

This study examined males and females in the pre-clinical sepsis model, with similar findings reported for both sexes.

Sepsis Cohort

RBCs from the day of ICU admission were obtained from human subjects enrolled in the MESSI cohort study at the University of Pennsylvania (IRB #808542).(1) Patients were eligible if they presented to the medical ICU with strongly suspected or confirmed infection and new or worsening organ dysfunction per historic Sepsis-2 "severe sepsis" criteria because enrollment preceded the publication of Sepsis-3.(30) Exclusion criteria included the primary reason for ICU admission being unrelated to infection, admission from a long-term acute-care hospital that might select for sepsis survivors or desire for exclusively palliative measures on ICU admission. Human subjects or their proxies provided informed consent.

Experimental animals

C57BL/6 mice were purchased from the Charles River Laboratories Inc. Tlr9 KO mice were produced by S. Akira and provided by E. Behrens (Children's Hospital of Philadelphia). Mice lacking erythrocyte Tlr9 ($Ery^{tlr9-/-}$) were generated by crossing ErGFPcre mice (a gift from U. Klingmüller, German Cancer Research Center) and Tlr9 KO Conditional mice (obtained from the European Mutant Mouse Archive). Genotype was confirmed through PCR amplification with the primers listed in Supplemental Table 3. All experimental procedures were performed on 8- to

12-week-old mice. Littermate controls were used in all experiments where Ery$^{tlr9-/-}$ mice were used.

Reagents

Bacterial genomic DNA was obtained from ATCC (25923D-5 for *S. aureus* subsp. *aureus* strain Seattle 1945 and 47085D-5 for *P. aeruginosa* strain PAO1-LAC, 700721D-5 for *K. pneumoniae* strain MGH78578). *Legionella pneumophila* was a kind gift from Dr. Sunny Shin (University of Pennsylvania). The corresponding genomic DNA was extracted using a DNeasy kit (Qiagen). IDT synthesized ODN1826 (CpG).

Macrophage isolation

WT mice were injected with 3mL Brewer's thioglycollate media intraperitoneally to obtain thioglycollate-elicited macrophages. After four days, mice were sacrificed via CO_2, and peritoneal lavage was aseptically collected by injecting and aspirating 5mL RPMI-1640 media in the peritoneum twice. The lavage was strained through a 70μm cell strainer, and the cells were adhered to a tissue culture-treated dish for 1hr at 37ºC in D10 media (DMEM supplemented with 10% FBS, 1% Pen/Strep, and 1% L-glutamine). Non-adherent cells were removed by washing three times with PBS (with calcium/magnesium). Adherent macrophages were lifted with a cell scraper and seeded onto 24-well plates at 250,000 cells per well overnight at 37ºC in D10 media. Macrophages were washed with PBS once before incubation with RBCs. In some experiments, macrophages were seeded onto sterile 12mm coverslips in 24-well plates.

In vitro DNA delivery by RBCs

Freshly isolated, leukoreduced RBCs were incubated with DNA at the ratio of 10ng bacterial DNA to 10^7 RBCs in 200µL DMEM for 4hr at 37ºC on a nutator. 25µg/mL ODN1826 was used as a control. All binding reactions were carried out in DNA LoBind tubes (Eppendorf). Subsequently, the DNA-RBC mixture was added to macrophages and incubated at 37ºC for 4hr. The supernatant containing RBCs were harvested and frozen at -80ºC for ELISA. To evaluate hemolysis, 60µL of the supernatant was centrifuged at 800g for 5min, and 50µL of the clarified supernatant was used to quantify cell-free hemoglobin using QuantiChrome hemoglobin assay according to the manufacturer's instructions.

Flow Cytometry

To evaluate the expression of TLR9 in myeloid cells and neutrophils, flow cytometry was performed. Whole blood was collected from WT and Ery$^{tlr9-/-}$ mice by cardiac puncture then centrifuged for 10 minutes at 3000g. Plasma was aspirated, and the buffy coat was collected. RBCs in the buffy coat were lysed using ACK lysis solution. Following red cell lysis, 10^6 cells were washed then treated with Fc block (Biolegend, Cat#101319) for 30 minutes on ice. Surface staining was performed with either CD11b (Biolegend, Clone M1/70, Cat #01251) or Ly6G (Biolegend, Clone 1A8, Cat #127626) antibodies for 30 minutes on ice. Cells were washed twice, then fixed and permeabilized using BD Cytofix/Cytoperm solution (BD Biosciences, Cat #554714) for 20 minutes at room temperature. Samples were washed then intracellularly stained for TLR9 (Biolegend, Clone S18025A, Cat #159103) for 40 minutes on ice. Following staining, cells were washed, resuspended in FACS buffer, and flow cytometry was performed using a LSR Fortessa cytometer (BD Biosciences). Analysis was performed using FlowJo Software.

DNA binding by murine RBCs

RBCs were isolated as previously described.[3] RBCs were incubated with 1ng of bacterial DNA (bDNA) in 200µL PBS in DNA lo-bind tube (Eppendorf) on a nutator at 37ºC for 2hr. The RBCs were then separated from the supernatant using sucrose gradient centrifugation (30% sucrose cushion, 13,000g for 5 min). The isolated red cell pellets were frozen at -80ºC until DNA extraction with a DNeasy blood kit (Qiagen). After DNA extraction, RBC-associated DNA was quantified with qPCR using either QuantStudio 6 or 7 (Applied Biosystems) using primers and probes listed in Supplemental Table 3. For *S. aureus* or *K. pneumoniae*, 16S multiplex primers were used in conjunction with the corresponding species-specific probe.(31)

In vivo DNA delivery by RBCs

Leukoreduced murine RBCs from WT or Tlr9 KO mice were washed with PBS and concentrated to a hematocrit of 40%. 160µL of the RBCs were mixed with 50µg ODN1826 at 40µL and transfused into recipient mice intravenously. After 6hr, blood was harvested via cardiac puncture, and plasma cytokines were quantified by ELISA. Livers were fixed in formalin and processed for histology as described below.

Cecal slurry-induced sepsis

Ery$^{tlr9-/-}$ mice and their littermates controls were used. Cecal slurry was generated as previously described and injected at 2mg/kg intraperitoneally.(1) Body temperature was monitored using an infrared thermometer at specific time points after CS injection (2, 4, 6, and 24 hours), with a detection limit of 88°F. Transient hypothermia was defined as mice that developed a low temperature (≤88°F) at any of the early time points (2, 4, or 6 hours) but recovered to >90°F by

24 hours. Persistent hypothermia was defined as mice with sustained low temperatures (remaining ≤88°F at 24 hours). At the indicated time (6 or 24 hrs after CS or control), mice were euthanized with 80 mg/kg ketamine and 10 mg/kg xylazine. Blood was collected via cardiac puncture with heparinized syringes. Tissues were excised and stored in TRIzol (Ambion), 10% buffered formalin acetate or PBS.

Quantification of tissue bacterial load was performed on the same day as necropsy. Tissues were weighed prior to storing in PBS and then homogenized and serially diluted in PBS. 10μL of each dilution was plated onto brain-heart infusion agar in triplicates and incubated at 37ºC for 24hr, and bacterial colonies were counted. Bacterial dissemination was defined as > 10^5 CFU/tissue. Isolation of RBCs for bound bacteria quantification were purified as previously described using TER119 beads. To generate RBC smears, 5μL of packed blood was spread onto SuperFrost Plus microscope slide. The slides were then air-dried and stained using DiffQuik.

Histology scoring criteria

For histology, lungs were vacuum expanded overnight in formalin. Spleens and liver were fixed overnight in formalin. Tissues were then processed for paraffin sectioning and scoring by the Comparative Pathology Core of the University of Pennsylvania School of Veterinary Medicine. Histopathological examination was performed blinded by a veterinary pathologist. 20 fields of 400X tissue sections were evaluated for histology criteria listed in Supplemental Table 1. As no validated sepsis scoring system exists for the liver and spleen, all histological findings were scored in a semiquantitative manner based on severity per International Harmonization of Nomenclature and Diagnostic Criteria (INHAND) recommendations. Criteria considered

common findings in sepsis were then weighted higher than less specific lesions and common background changes.

RBC smear scoring

The blood smear score was determined by two blinded reviewers using an Olympus BX41 microscope at 40X magnification. Five random fields of view were assessed for each mouse. Echinocytes, bite cells, rouleaux, and teardrop cells were considered 'abnormal' RBCs. If over 50% of the field-of-view contained abnormal cells, then that field-of-view was given a score of one. If less than 50% of the field-of-view contained abnormal cells, then that field-of-view was given a score of zero. Once five random fields-of-view were scored for a given mouse, then a total score from zero to five was determined by summing the individual field-of-view scores for the mouse. A total score of zero indicates a low abnormality, while a total score of five indicates a very high abnormality.

Hemoglobin Assays

Hemoglobin assays were performed utilizing a commercially available kit (QuantiChrom Hemoglobin Assay, BioAssay Systems, Cat#DIHB-250). RBCs from naive WT and Ery$^{tlr9-/-}$ mice were isolated using magnetic anti-Ter119 beads (Miltenyi Biotec). Cells were saved as 10^7 cell pellets at -80 °C until use. To measure hemoglobin in RBCs, 10^7 cells were lysed in 50ul of water prior to the assay. For measurement of cell free hemoglobin in the plasma, the plasma from animals that received either 24-hour D5W or cecal slurry injection was saved at -80°C until time of assay. Plasma was thawed, then diluted 1:4 in water and assayed following kit instructions.

qRT-PCR

RNA was extracted from tissues in TRIzol (Ambion) using a RNeasy Plus kit (Qiagen) following the manufacturer's protocol. RNA was reverse transcribed into cDNA using a High-Capacity cDNA kit (Applied Biosystems). DNA on RBC samples was extracted with a DNeasy blood and tissue kit (Qiagen). RBCs were isolated and manually enumerated as previously described.(1) Gene expression was quantified with PowerUp SYBR Green Master Mix or TaqMan Fast Universal PCR Master Mix (Applied Biosystems) with primers or probes listed in Supplemental Table 3. For quantification of 16S rDNA on murine RBCs, a 1:5 dilution of DNA was used for qPCR.

Cytokine quantification

Cytokine expression in mouse plasma was quantified with a custom U-plex cytokine panel (Meso Scale Discovery) of the following analytes: IL-6, TNFα, IL-1β, IL-10, IL-12p70, IL-27p28, and IFNγ or standard ELISA according to manufacturer's protocol (DuoSet, R&D Systems). If a value was below the limit of detection, it was denoted with a zero.

Isolation of F4/80$^+$ red pulp macrophages

F4/80+ cells were magnetically isolated with F4/80-bead (Miltenyi Biotec) following manufacturer's protocol.

Bioinformatics

We performed unsupervised learning to identify clusters within the data. We applied agglomerative (hierarchical) clustering to the Z-normalized cytokine data with using a complete linkage to produce heatmaps, and dimensional reduction with uniform manifold approximation and projection (UMAP). For this latter approach, we used the Python package *umap-learn* to calculate the projection using the nine cytokines as input features. To visualize how the underlying features contributed to the visualized clusters we fit a kernel density estimator to the UMAP coordinates weighted by the log of the features Z-scores to produce contour maps. Graphics were generated using a combination of the Seaborn and Matplotlib packages.

16S qPCR on human RBCs

Red blood cells were isolated using magnetic anti-Glycophorin A (GPA) beads (Miltenyi Biotec) and then manually enumerated at aliquoted as 10^7 RBCs and saved at -80C until extraction. DNA extraction was performed using a DNeasy blood kit (Qiagen) and DNA was eluted in 152µL buffer AE. 16s DNA was evaluated using the Universal 16s primers and probes listed in Supplemental Table 3, PCR was run to 50 cycles and quantified using QuantStudio 6 or 7 (Applied Biosystems). When converting cycle thresholds to copy numbers, undetermined values were reported as "1". AE buffer and ddwater negative controls were run with each qPCR reaction. For 16S sequencing, ddwater, AE buffer, and AE buffer run through DNA isolation columns were included as negative controls. Three individual samples for each negative control were provided to the sequencing core. In addition to these controls, DNA-free water and gene block negative controls were included in the sequencing.

16S sequencing and analysis

The 16S rRNA amplicon sequences were initially analyzed using QIIME2 (qiime2.org, version 2021.2). DADA2 was used for quality control, denoising, and amplicon sequence variant (ASV) creation.(32) ASV with less than 10 hits across samples were filtered out. A naïve Bayesian classifier was used to assign taxonomy against the Greengenes (version 13.8) database. We performed microbial ecology analysis using the *vegan* package 2.6-1 and in *R* 4.2.2.(33-35) For relative abundance and ordination analysis, samples were normalized to the percent of total reads and we restricted analysis to ASVs that were present at greater than 1% of the sample population. All ASVs were included in diversity analysis. Direct community similarity comparisons were performed using the Bray-Curtis similarity index. We performed ordinations using Principal Component Analysis on Hellinger-transformed normalized OTU tables generated using Euclidean distances(36). We determined significance of differences in community composition using PERMANOVA (*adonis*) with 10,000 permutations using Euclidean distances. We compared means via Student's T test and ANOVA with Holm-Sidak's multiple comparisons test as appropriate.

Statistics Summary

GraphPad Prism was used to perform all statistical analysis with the exception of 16S sequencing analysis and Bioinformatics analysis described above. A two-tailed T-test or Mann-Whitney U-test was used to compare between 2 groups depending on normality. One-way ANOVA or Kruskal-Wallis was used to compare more than two groups depending on normality, followed by indicated post hoc tests. A P value less than 0.05 was considered significant.

Study Approval

All studies involving animals were approved by the University of Pennsylvania IACUC. For studies involving human subjects, all studies were approved by the University of Pennsylvania IRB. Patients or their proxies provided written informed consent.

Data Availability: All data are available in the main text and supplementary materials. A supporting data values file can be found online. Raw sequence data is uploaded to the NCBI, Bio Project, Accession number PRJNA1068992.

Author contributions: Experiments were conceived and designed by LKML and NSM. Experiments were performed by LKML, KAE, ML, EAO, LS, and JSJ. Data were analyzed by LKML, JSJ, CVC, JM, NK, NY, NJM, PR, RPD and NSM. NSM and RPD wrote the paper.

Acknowledgments:

Funding:

NIH R01 HL126788 (NSM)

NIH R21 AI166813 (NSM)

Penn Synergy Program, Penn Center for Precision Medicine (NSM)

References Cited

1. Lam LKM, Murphy S, Kokkinaki D, Venosa A, Sherrill-Mix S, Casu C, et al. DNA binding to TLR9 expressed by red blood cells promotes innate immune activation and anemia. *Sci Transl Med.* 2021;13(616):eabj1008.
2. Langelier C, Fung M, Caldera S, Deiss T, Lyden A, Prince BC, et al. Detection of Pneumonia Pathogens from Plasma Cell-Free DNA. *Am J Respir Crit Care Med.* 2020;201(4):491-5.
3. Yang H, Haidar G, Al-Yousif NS, Zia H, Kotok D, Ahmed AA, et al. Circulating microbial cell-free DNA is associated with inflammatory host-responses in severe pneumonia. *Thorax.* 2021;76(12):1231-5.
4. Bongers KS, Chanderraj R, Woods RJ, McDonald RA, Adame MD, Falkowski NR, et al. The Gut Microbiome Modulates Body Temperature Both in Sepsis and Health. *Am J Respir Crit Care Med.* 2022.
5. Tsuchida T, Wada T, Mizugaki A, Oda Y, Kayano K, Yamakawa K, et al. Protocol for a Sepsis Model Utilizing Fecal Suspension in Mice: Fecal Suspension Intraperitoneal Injection Model. *Frontiers in Medicine.* 2022;9.
6. Lee MJ, Kim K, Jo YH, Lee JH, and Hwang JE. Dose-dependent mortality and organ injury in a cecal slurry peritonitis model. *J Surg Res.* 2016;206(2):427-34.
7. Larsen R, Gozzelino R, Jeney V, Tokaji L, Bozza FA, Japiassu AM, et al. A central role for free heme in the pathogenesis of severe sepsis. *Sci Transl Med.* 2010;2(51):51ra71.
8. Luo B, Gan W, Liu Z, Shen Z, Wang J, Shi R, et al. Erythropoeitin Signaling in Macrophages Promotes Dying Cell Clearance and Immune Tolerance. *Immunity.* 2016;44(2):287-302.
9. Interleukin-6 Receptor Antagonists in Critically Ill Patients with Covid-19. *New England Journal of Medicine.* 2021;384(16):1491-502.
10. Kalil AC, Patterson TF, Mehta AK, Tomashek KM, Wolfe CR, Ghazaryan V, et al. Baricitinib plus Remdesivir for Hospitalized Adults with Covid-19. *New England Journal of Medicine.* 2020;384(9):795-807.
11. Dexamethasone in Hospitalized Patients with Covid-19. *New England Journal of Medicine.* 2020;384(8):693-704.
12. Meyer NJ, Reilly JP, Anderson BJ, Palakshappa JA, Jones TK, Dunn TG, et al. Mortality Benefit of Recombinant Human Interleukin-1 Receptor Antagonist for Sepsis Varies by Initial Interleukin-1 Receptor Antagonist Plasma Concentration. *Crit Care Med.* 2018;46(1):21-8.
13. Nandi M, Jackson SK, Macrae D, Shankar-Hari M, Tremoleda JL, and Lilley E. Rethinking animal models of sepsis - working towards improved clinical translation whilst integrating the 3Rs. *Clin Sci (Lond).* 2020;134(13):1715-34.
14. Bhavani SV, Semler M, Qian ET, Verhoef PA, Robichaux C, Churpek MM, et al. Development and validation of novel sepsis subphenotypes using trajectories of vital signs. *Intensive Care Med.* 2022;48(11):1582-92.
15. Hotz MJ, Qing D, Shashaty MGS, Zhang P, Faust H, Sondheimer N, et al. Red Blood Cells Homeostatically Bind Mitochondrial DNA through TLR9 to Maintain Quiescence and to Prevent Lung Injury. *Am J Respir Crit Care Med.* 2018;197(4):470-80.
16. Nakahira K, Kyung SY, Rogers AJ, Gazourian L, Youn S, Massaro AF, et al. Circulating mitochondrial DNA in patients in the ICU as a marker of mortality: derivation and validation. *PLoS Med.* 2013;10(12):e1001577; discussion e.
17. Faust HE, Reilly JP, Anderson BJ, Ittner CAG, Forker CM, Zhang P, et al. Plasma Mitochondrial DNA Levels Are Associated With ARDS in Trauma and Sepsis Patients. *Chest.* 2020;157(1):67-76.
18. Kitsios GD, Bain W, Al-Yousif N, Duttagupta R, Ahmed AA, McVerry BJ, et al. Plasma microbial cell-free DNA load is associated with mortality in patients with COVID-19. *Respiratory Research.* 2021;22(1):24.
19. Lleo MM, Ghidini V, Tafi MC, Castellani F, Trento I, and Boaretti M. Detecting the presence of bacterial DNA by PCR can be useful in diagnosing culture-negative cases of infection, especially in patients with suspected infection and antibiotic therapy. *FEMS Microbiol Lett.* 2014;354(2):153-60.
20. Gosiewski T, Ludwig-Galezowska AH, Huminska K, Sroka-Oleksiak A, Radkowski P, Salamon D, et al. Comprehensive detection and identification of bacterial DNA in the blood of patients with sepsis and healthy volunteers using next-generation sequencing method - the observation of DNAemia. *European Journal of Clinical Microbiology & Infectious Diseases.* 2017;36(2):329-36.

21. Neyton LPA, Sinha P, Sarma A, Mick E, Kalantar K, Chen S, et al. Host and Microbe Blood Metagenomics Reveals Key Pathways Characterizing Critical Illness Phenotypes. *Am J Respir Crit Care Med.* 2024.
22. Dickson RP, Singer BH, Newstead MW, Falkowski NR, Erb-Downward JR, Standiford TJ, et al. Enrichment of the lung microbiome with gut bacteria in sepsis and the acute respiratory distress syndrome. *Nat Microbiol.* 2016;1(10):16113.
23. Singer BH, Dickson RP, Denstaedt SJ, Newstead MW, Kim K, Falkowski NR, et al. Bacterial Dissemination to the Brain in Sepsis. *Am J Respir Crit Care Med.* 2018;197(6):747-56.
24. Klingensmith NJ, and Coopersmith CM. The Gut as the Motor of Multiple Organ Dysfunction in Critical Illness. *Crit Care Clin.* 2016;32(2):203-12.
25. Bhanji S, Williams B, Sheller B, Elwood T, and Mancl L. Transient bacteremia induced by toothbrushing a comparison of the Sonicare toothbrush with a conventional toothbrush. *Pediatr Dent.* 2002;24(4):295-9.
26. Ogden HB, Fallowfield JL, Child RB, Davison G, Fleming SC, Delves SK, et al. Influence of aerobic fitness on gastrointestinal barrier integrity and microbial translocation following a fixed-intensity military exertional heat stress test. *European Journal of Applied Physiology.* 2020;120(10):2325-37.
27. Lockhart PB, Brennan MT, Sasser HC, Fox PC, Paster BJ, and Bahrani-Mougeot FK. Bacteremia associated with toothbrushing and dental extraction. *Circulation.* 2008;117(24):3118-25.
28. Thevaranjan N, Puchta A, Schulz C, Naidoo A, Szamosi JC, Verschoor CP, et al. Age-Associated Microbial Dysbiosis Promotes Intestinal Permeability, Systemic Inflammation, and Macrophage Dysfunction. *Cell Host Microbe.* 2017;21(4):455-66.e4.
29. He Y, Cheng C, Liu Y, Chen F-M, Chen Y, Yang C, et al. Intravenous Senescent Erythrocyte Vaccination Modulates Adaptive Immunity and Splenic Complement Production. *ACS Nano.* 2023.
30. Singer M, Deutschman CS, Seymour CW, Shankar-Hari M, Annane D, Bauer M, et al. The Third International Consensus Definitions for Sepsis and Septic Shock (Sepsis-3). *Jama.* 2016;315(8):801-10.
31. Liu CF, Shi XP, Chen Y, Jin Y, and Zhang B. Rapid diagnosis of sepsis with TaqMan-Based multiplex real-time PCR. *Journal of clinical laboratory analysis.* 2018;32(2).
32. Callahan BJ, McMurdie PJ, Rosen MJ, Han AW, Johnson AJA, and Holmes SP. DADA2: High-resolution sample inference from Illumina amplicon data. *Nature Methods.* 2016;13(7):581-3.
33. Oksanen JF, Blanchet G, Kindt R, Legendre P, Minchin PR, O'Hara RB, et al.; 2012.
34. R Core Team. Vienna, Austria: R Foundation for Statistical Computing; 2013.
35. Wang Y, Naumann U, Wright ST, and Warton DI. mvabund- an R package for model-based analysis of multivariate abundance data. *Methods Ecol Evol.* 2012;3(3):471-4.
36. Legendre P, and Gallagher ED. Ecologically meaningful transformations for ordination of species data. *Oecologia.*129(2):271-80.

Figure 1

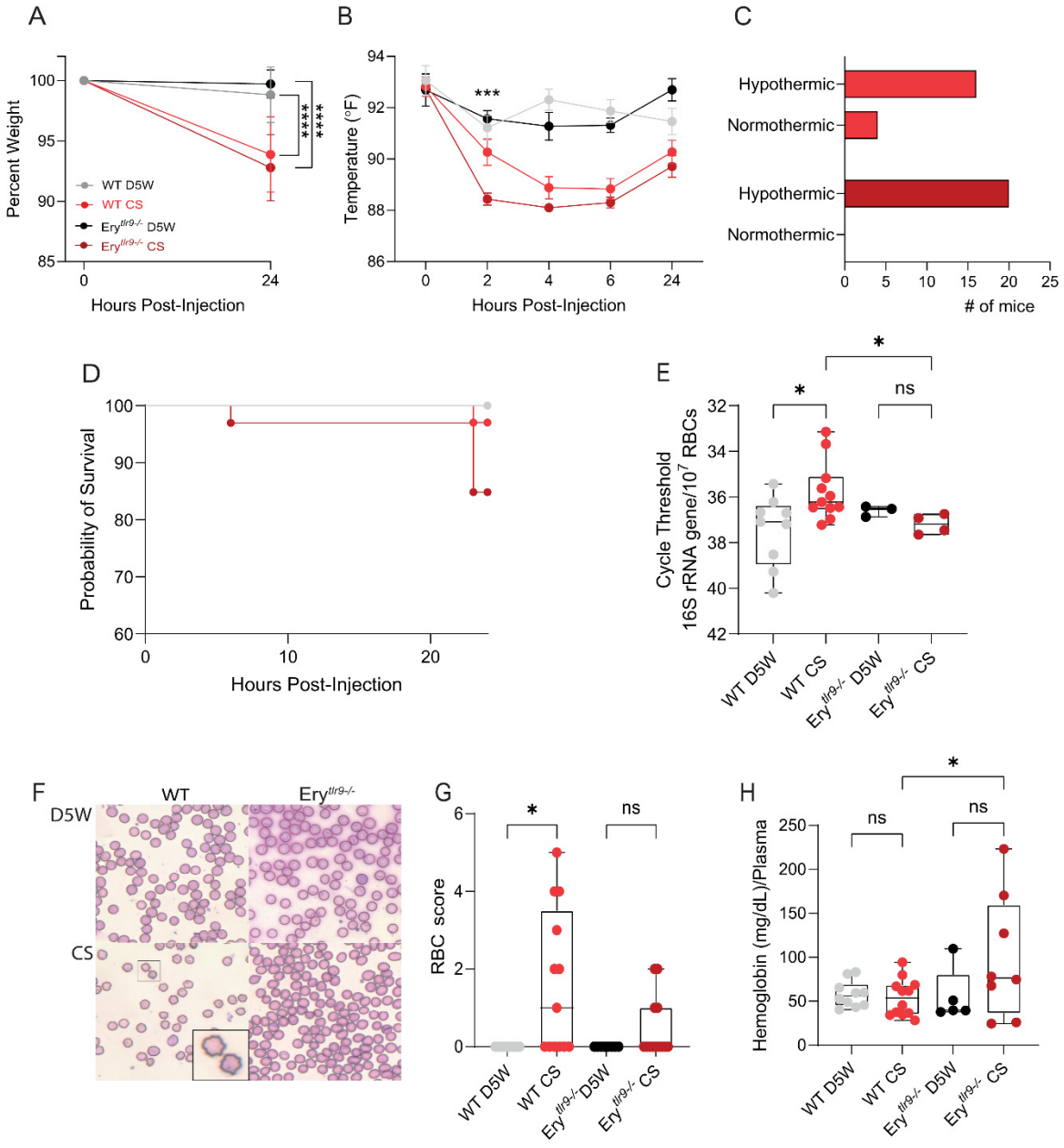

Figure 1. RBCs from WT but not Ery$^{tlr9-/-}$ mice acquire microbial DNA and demonstrate morphologic changes during sepsis. Ery$^{tlr9-/-}$ or WT littermates were injected with CS or D5W and monitored for 24 hours. (**A**) Weight change and differences between groups were analyzed by ANOVA with Sidak's multiple comparisons, ****P<0.0001 for WT D5W v WT CS and Ery$^{tlr9-/-}$ D5W v Ery$^{tlr9-/-}$ CS, WT CS v Ery$^{tlr9-/-}$ CS= ns, n=20-30 mice per group. (**B**) Temperature profiles of injected mice, 88°F was the lower limit of detection, ANOVA with Sidak's multiple comparison analysis, ***P=0.002 between CS-injected groups at 2 hours, P=0.005 between Ery$^{tlr9-/-}$ D5W and Ery$^{tlr9-/-}$ CS, n=9-20 mice per group. (**C**) Hypothermic state of the mice by strain at 24 hours, P=0.035 by chi-square test. (**D**) Kaplan Meier survival with log-rank comparison, P=0.031 between all groups, P=0.08 WT CS v Ery$^{tlr9-/-}$ CS. (**E**) RBC-associated 16S

rRNA gene on murine RBCs was quantified 6 hours following CS-induced sepsis. One-way Kruskal-Wallis test with Dunn's multiple comparisons, n=3-11, *P =0.042 WT D5W v WT CS, *P=0.044 WT CS v Ery$^{tlr9-/-}$ CS. (**F**) RBCs from WT or Ery$^{tlr9-/-}$ mice 24 hours following D5W or CS injection, insert shows echinocytic RBCs observed in the WT CS injected mice(**G**) RBC score (number of echinocytes and altered RBCs/hpf), P= 0.013, WT D5W v WT CS, n=8-14 from 3 independent studies. **(H)** Cell-free hemoglobin 24 hours following CS injection. Differences between groups were measured using one-way ANOVA with Sidak's multiple comparisons test. P=0.044 for WT CS v Ery$^{tlr9-/-}$ CS, P=ns for all other comparisons.

Figure 2

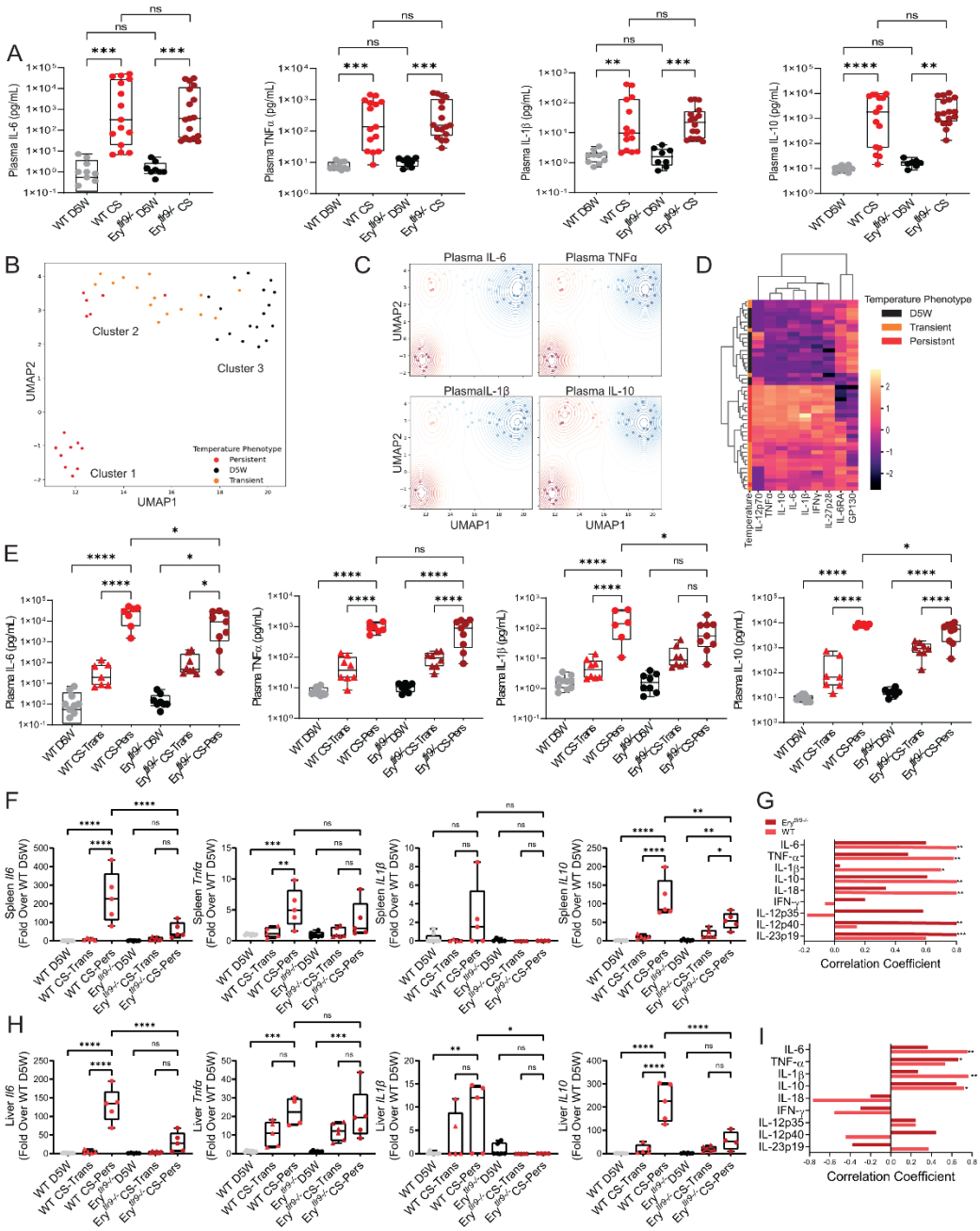

Figure 2. Plasma cytokine and gene expression in WT and Ery$^{tlr9-/-}$ mice following CS injection. (**A**) Plasma cytokines 24 hours following CS or D5W injection, n=8-17 per group from 4 independent studies. (**B**) Uniform manifold approximation and projection derived from the nine measured plasma cytokine concentrations colored by whether they developed persistent or transient hypothermia or were controls (D5W). (**C**) Weighted kernel density estimation illustrating relative concentration (red higher, blue lower) of the cytokines in each cluster. (**D**) Heatmap of cytokines structured with agglomerative clustering similarly illustrating the correlation between cytokine concentration and hypothermia. (**E**) Plasma cytokines 24 hours after CS or D5W injection, plasma cytokines stratified based on hypothermic state.

Trans=transient hypothermia, Pers=persistant hypothermia at 24 hours following injection. (**F**) Splenic expression of immune genes stratified based on hypothermic state and (**G**) Association between bacterial load and tissue cytokines in the spleen, Spearman's correlation, an asterisk denotes significant correlation between tissue cytokine and bacterial load. (**H**) Hepatic expression of immune genes stratified based on hypothermic state and (**I**) Association between bacterial load and tissue cytokines in the liver, Spearman's correlation, an asterisk denotes a significant correlation between tissue cytokine and bacterial load. Differences between groups were analyzed by one-way Kruskal-Wallis test with Dunn's post-hoc in (**A**) and one-way ANOVA with Holm-Sidak test in (**E**), (**F**), and (**H**), n=4-8 per temperature stratified group from 4 independent studies in (**F**-**I**). *P <0.05, **P< 0.01, ***P<0.001, ****P<0.0001.

Figure 3

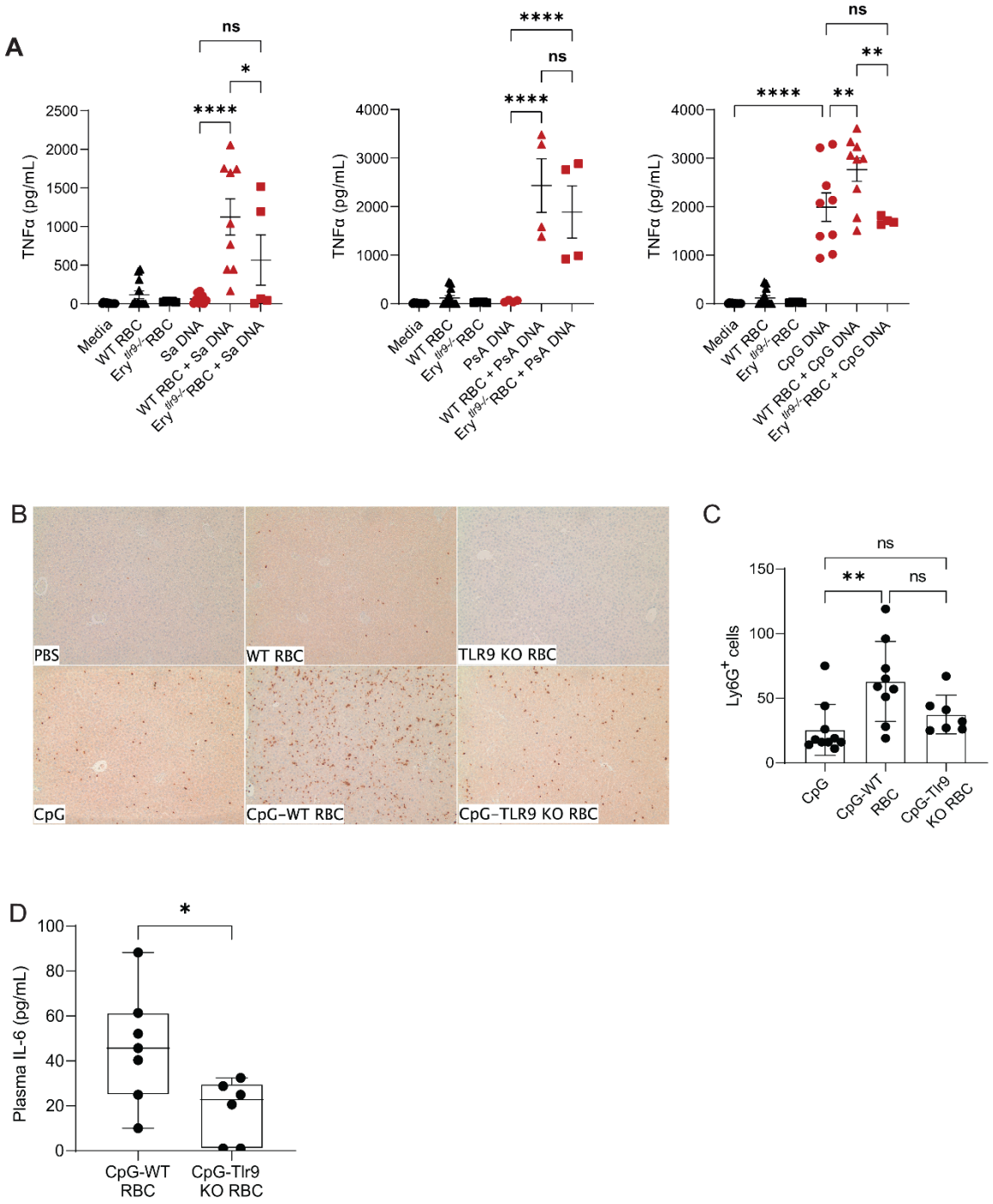

Figure 3. Murine RBCs acquire and deliver DNA to remote organs and immune cells (**A**) TNFα production by peritoneal macrophages four hours following treatment with media, RBCs (WT or Ery$^{tlr9-/-}$), or RBCs pre-incubated with *S. aureus* genomic DNA (Sa DNA), *P. aeruginosa* DNA (PsA), or CpG-ODN 1826. Results from 2-4 independent studies are shown. Differences between groups were analyzed with one-way ANOVA followed by Holm-Sidak post-hoc

comparison with *P<0.05, **P<0.01 and ****P<0.0001. (**B**) Ly6G staining of liver sections 6 hours following transfusion of CpG or CpG-treated RBCs and (**C**) quantification of $Ly6G^+$ cells. (**D**) Plasma IL-6 6 hours following transfusion of mice with CpG-treated WT or TLR9 KO RBCs. Differences between groups were analyzed with Kruskal-Wallis test and Dunn's posthoc analysis in (**B**) and unpaired t-test in (**D**), n=6-10 from 2 independent experiments, *P<0.05 and **P<0.01.

Figure 4

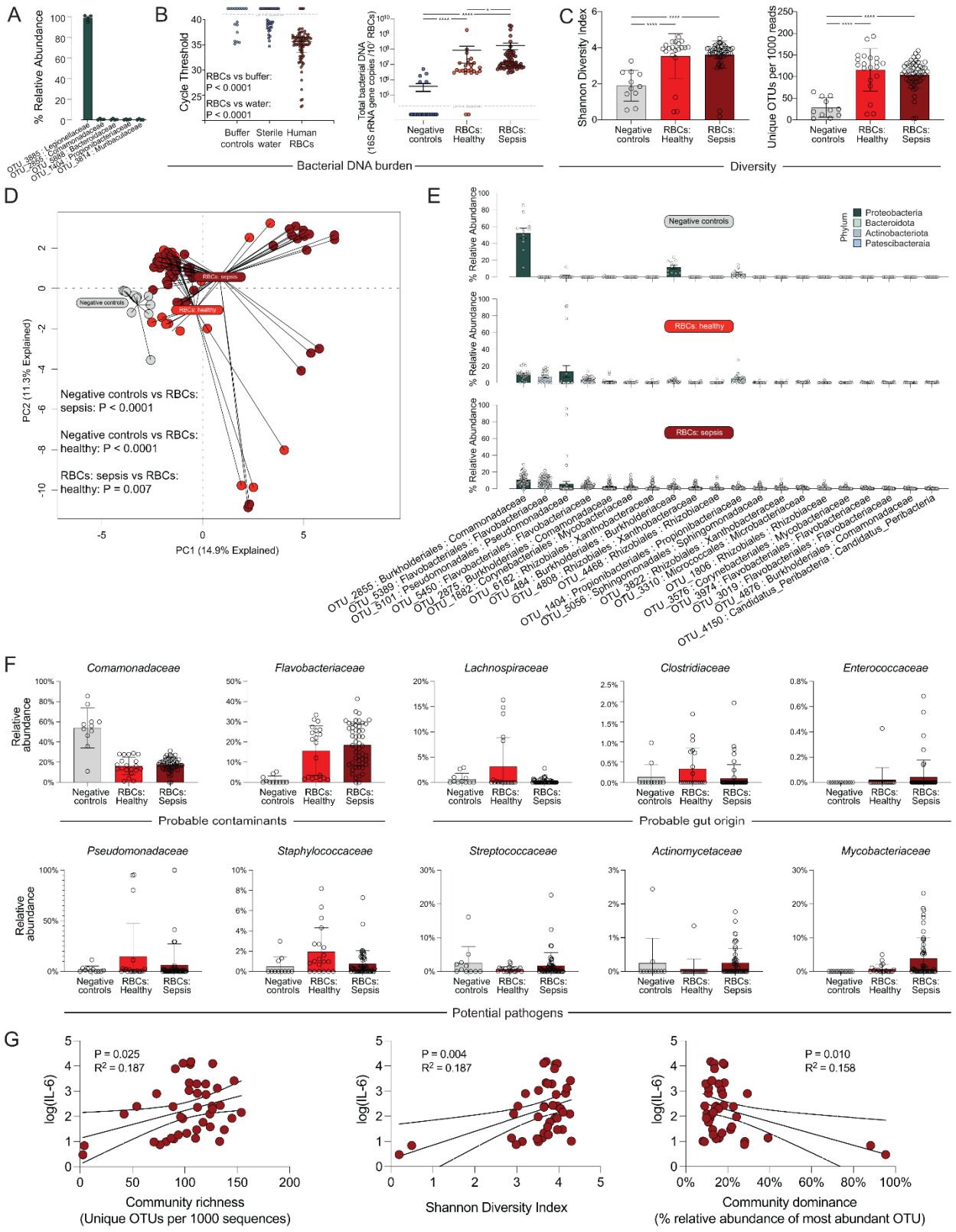

Figure 4. Analysis of bacterial DNA associated with red blood cells. (**A**) We incubated red

blood cells with Legionella sp. then performed 16S rRNA gene amplicon sequencing on the red blood cells. RBC-associated DNA was dominated by Legionella-classified amplicons (97.5%). (**B**) We quantified RBC-associated bacterial DNA using qPCR of the 16S rRNA gene. Human RBCs had a greater quantity of bacterial DNA than did negative control specimens, and RBCs from humans with sepsis had more bacterial DNA than healthy volunteers, n=27 healthy donors and 64 patients with sepsis. (**C**) RBC-associated bacterial DNA contained a greater diversity of bacterial taxa than did negative control specimens. Negative control specimens include ddwater, AE buffer, AE buffer run through DNA isolation columns, and DNA free water. (**D**) Bacterial taxa detected in RBCs (both in health and sepsis) were distinct from those of negative control specimens and distinct from each other. (**E**) Rank abundance analysis demonstrated the influence of some contaminant taxa on RBC taxa (e.g., Comamonadaceae) as well as distinct taxa within RBC specimens not detected in negative control specimens. (**F**) Direct comparison of prominent bacterial families across negative controls and RBC from healthy and septic patients. (**G**) Among patients with sepsis, the acute inflammatory cytokine IL-6 was positively correlated with RBC-bound bacterial DNA diversity. Unadjusted association of plasma IL-6 with community richness, Shannon index, and community dominance are shown. When adjusted for APACHE score and vasopressor use, the association remained significant. Adjusted for APACHE, P=0.039,0.012, and 0.024 for richness, Shannon index, and community dominance. Adjusting for vasopressor use, P=0.04, 0.006, and 0.013 for richness, Shannon index, and community dominance. n=20 healthy controls and 51 patients with sepsis for C-G.

Table 1. Organ dissemination stratified by strain. Data are shown as number observed (%). Comparisons shown were calculated by chi-square tests. For the blood dissemination, n=18 for WT and 15 for Ery$^{tlr9-/-}$.

	WT	**Ery$^{tlr9-/-}$**	***P***
	(n=19)	**(n=16)**	
Blood	8 (44%)	11 (65%)	0.09
Spleen	10 (53%)	14 (88%)	0.03
Liver	13 (68%)	15 (94%)	0.06
Lung	13 (68%)	13 (81%)	0.39

Table 2. MESSI cohort patient characteristics.

	n (%), median [IQR]
Age (median, IQR)	61 (49, 69)
Gender (%female)	17 (33%)
APACHE III score (median, IQR)	85 (63, 138)
Admission source:	
ED	28 (55%)
Floor Transfer	19 (37%)
OSH transfer	4 (8%)
Required vasopressors 1st 24h	32 (62%)
ARDS	15 (29%)
Lung source of sepsis	29 (57%)
30 day mortality	19 (37%)
90 day mortality	27 (53%)
Blood Culture Positive	17 (33%)